

Sebastian Fischer · Harald Beyer · Ralf Janke  
Jürgen Wilde

# The influence of package-induced stresses on moulded Hall sensors

Received: 24 June 2004 / Accepted: 14 February 2005  
© Springer-Verlag 2005

**Abstract** The output signals of moulded Hall sensors show changes in offset and sensitivity when the devices are affected by changing temperatures. This behaviour is a result of the differences in the thermal expansion behaviour of the package materials and is also affected by their time-dependent, viscous material properties. The stresses affected to the sensor's sensitive layer will become effective via the piezo-Hall-effect as well as via piezo-resistivity which both change the sensitivity and the offset of the sensor's output voltage. For modelling the stress in the sensitive area correctly it is indispensable to consider the visco-elastic and the visco-plastic behaviour of the materials constituting the package. Especially for very accurate sensors or components operating in harsh environments these effects must be regarded. In this work we investigate the thermo-mechanical stresses, which are induced in the sensitive layer of a moulded Hall sensor during the assembly process, the investigations were based mainly on finite-elements-simulations.

## 1 Introduction

Hall sensors are widely used for position detection. Especially in automotive applications the requirements to the sensor device are rather high regarding the offset and sensitivity accuracy over temperature cycles. Due to the piezo properties of the Hall layer the sensors are very sensitive to mechanical stress, which will change the offset and the sensitivity of the device significantly.

The relation between the electric field  $\vec{E}$ , the current density  $\vec{J}$  and the magnetic flux density  $\vec{B}$  in a cubic

crystal like silicon can be expressed as (Fischer et al. 2004; Manic et al. 2000):

$$\vec{E} = \rho \vec{J} - (R_H \vec{B}) \times \vec{J} \quad (1)$$

where  $R_H$  and  $\rho$  are the Hall coefficients and the resistivity, respectively, and both are functions of the mechanical stress within the sensitive layer. Their relative changes are defined by

$$\frac{\Delta \rho_{ij}}{\rho_0} = \sum_{kl} \pi_{ijkl} \sigma_{kl} \quad (2)$$

and

$$\frac{\Delta R_{ij}}{R_0} = \sum_{kl} P_{ijkl} \sigma_{kl} \quad (3)$$

where  $\sigma_{kl}$  is the tensor of the mechanical stress,  $\pi_{ijkl}$  and  $P_{ijkl}$  are the piezoresistive and the piezo-Hall coefficient tensors, respectively.

## 2 Assembly of moulded Hall sensors

A typical Hall sensor comprises the silicon chip, which is conductively glued on a leadframe and moulded into a epoxy or plastic moulding compound. Figure 1 displays a cross section of a leaded Hall sensor package. The top layer of the silicon chip contains the sensitive area.

Figure 2 shows a finite element model of a leaded Hall sensor device. The bonding wires have been neglected for this simulation.

Typical data for the materials, taken from several sources (see Table 1).

## 3 Variables of the simulation

When calculating the mechanical stress in the top silicon layer due to temperature changes a variety of parameters can be considered (Deier and Wilde 2003; Fischer et al.

S. Fischer (✉) · J. Wilde  
IMTEK, University of Freiburg, Freiburg, Germany  
Email: sfischer@imtek.de

H. Beyer · R. Janke  
Micronas GmbH, Freiburg, Germany

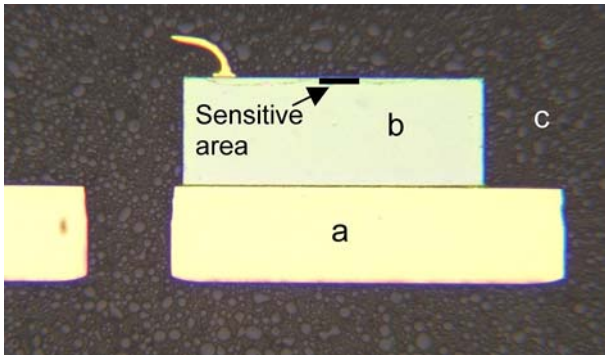


**Fig. 1** Cross section of a Hall sensor attached to a leadframe by a conductive adhesive and surrounded by a moulding compound, a part of the bonding wire can be seen; **a** leadframe; **b** silicon sensor chip, thickness 380  $\mu\text{m}$ ; **c** moulding compound

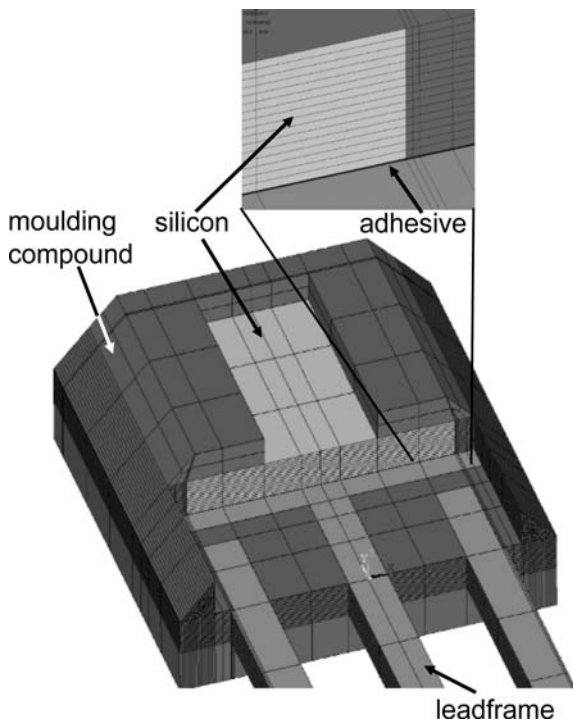


**Fig. 2** Example schematic of FE-simulation of a moulded Hall sensor in a leaded package, PTO-type

**Table 1**  $\alpha_1$  and  $\alpha_2$  are the coefficients of thermal expansion *below* and *above* the glass transition temperature

Material	Young's modulus (GPa)	CTE $\alpha_1$ ( $\text{K}^{-1}$ )	CTE $\alpha_2$ ( $\text{K}^{-1}$ )
Silicon	165	$2 \times 10^{-6}$	
Conductive adhesive	7.5	$6.5 \times 10^{-5}$	$13.5 \times 10^{-5}$
Leadframe	133	$1.7 \times 10^{-5}$	
Moulding compound	20	$1.2 \times 10^{-5}$	$4 \times 10^{-5}$

2004). Geometry as well as different material properties influence the stress field in the sensor as will be shown in the next paragraphs.

### 3.1 Geometry parameters

Geometry parameters, such as the thickness of the leadframe, the silicon, the bottom and top moulding compound thickness may have a significant influence on the stress field in the device. By changing these parameters, an optimized design can be found.

### 3.2 Temperature-dependent material parameters

Material properties such as Young's modulus and the coefficient of thermal expansion (CTE) reveal a strong temperature dependency. Figures 3 and 4 clarify that the mechanical properties of moulding compounds change significantly over the temperature range as well as between different moulding compounds. Two different compounds are displayed. Type a is a typical low-stress material whereas type b is a super-low-stress moulding compound. Polymers with a glass transition temperature  $T_g$  within the relevant temperature range show a substantial increase of the CTE in that temperature range.

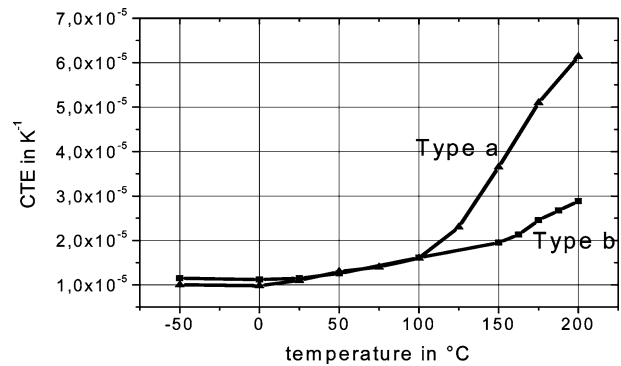


**Fig. 3** Temperature-dependent coefficients of thermal expansion of typical moulding compounds

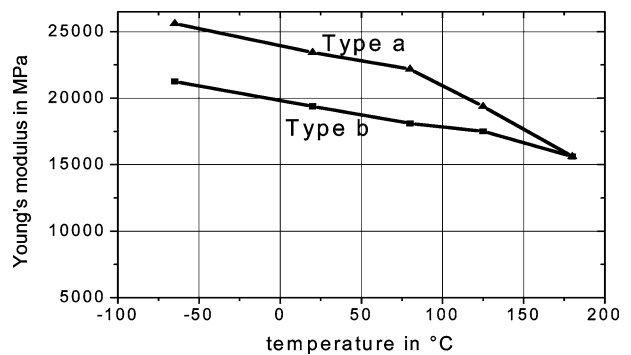


**Fig. 4** Temperature-dependent Young's moduli of typical low stress moulding compounds

The Young's modulus declines over temperature, but also a strong variation between different moulding compounds can be observed. Type a changes its slope to a sharper decrease of the elastic modulus at temperatures above 80°C whereas type b shows a stable slope over the entire temperature range.

### 3.3 Time-dependent material parameters

Epoxy moulding compounds exhibit time-dependent materials behaviour. The performed tests on epoxy moulding compounds demonstrate that the time-dependent mechanical behaviour is highly complex (Fig. 5). The test specimens were loaded and unloaded in three steps between 20 and 80 MPa. The resulting curves of normal strain over time indicate a spontaneous elastic deformation when bringing up the load. Holding the load over a time interval, a time-dependent increase of strain is found. Unloading will lead to a spontaneous elastic decrease of a large portion of strain and a small time-dependent decrease of strain. This reversible portion of deformation corresponds to viscoelasticity. In a material, which only exhibits elasticity plus viscoplastic (creep) behaviour, there will be no time-dependent decrease after unloading. Generally, the maximum total

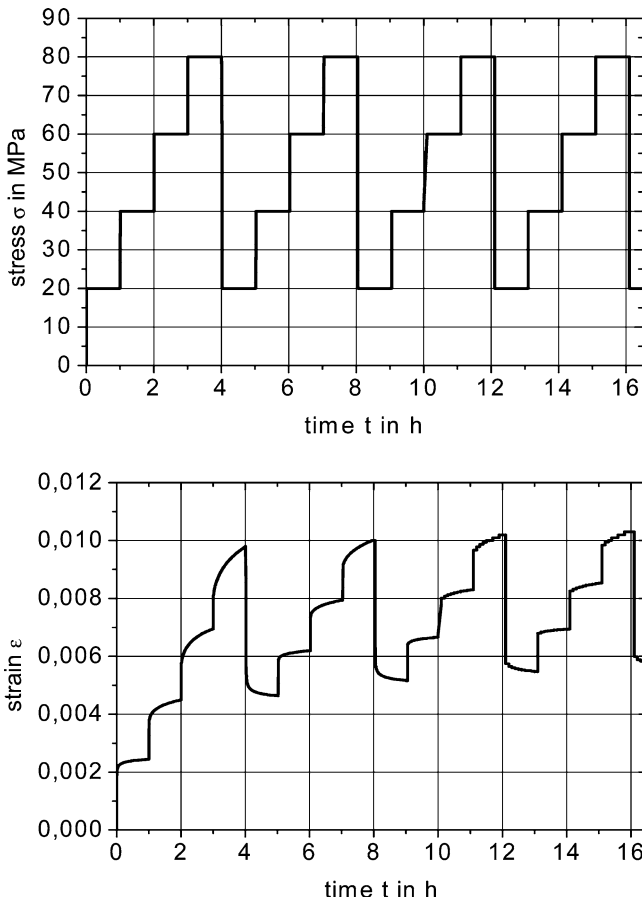


Fig. 5 Measured compressive strain in a low stress moulding compound under cyclic stress loading at  $T=150^{\circ}\text{C}$

strain is increasing slightly over time, which is a result of irreversible creep deformation. These strains correspond to viscoplastic strains.

Due to the complex materials behaviour a model is needed which is capable of modelling elastic, viscoelastic and also viscoplastic deformations.

Figure 6 shows a rheological model which is typically used for describing non-linearity and time-dependency of a system showing such a behaviour and describes the mechanical deformation of moulding compounds (Deier and Wilde 2003).

For modelling and calculating the stress in a package one needs to use a material model, which is implemented in a finite element program. In ANSYS the stress-viscoelastic strain behaviour is based on a materials model, which describes a time-dependent shear modulus  $G$ .

$$\sigma = \int_0^t 2G(t - \tau) \frac{d\epsilon}{d\tau} d\tau \quad (4)$$

where  $\sigma$  is the stress,  $\epsilon$  is the deviatoric part of strain, and  $G(t)$  is the shear modulus.

The shear relaxation kernel function is defined as a Prony series (5), with up to six Prony components. Each of these can be defined temperature-dependent.  $G_{\text{inf}}$  is the shear modulus at time infinity, the sum of  $G_{\text{inf}}$  and  $G_i$  is the elastic shear modulus.  $\phi_i$  is the time constant of relaxation. The stress-viscoplastic strain behaviour in ANSYS is based on Anand's law, which is suitable for modelling both primary and secondary creep (Fig. 7).

$$G(t, T) = G(T)_{\text{inf}} + \sum_{i=1}^n G(T)_i \exp\left(-\frac{t}{\phi(T)_i}\right) \quad (5)$$

$$\dot{\epsilon}_{\text{vp}} = A e^{\frac{-Q}{RT}} \left[ \sinh\left(\zeta \frac{\sigma}{S}\right) \right]^{1/m} \quad (6)$$

$$\dot{s} = \left[ h_0 (|B|)^a \frac{B}{|B|} \right] \dot{\epsilon} \quad \text{with } a < 1$$

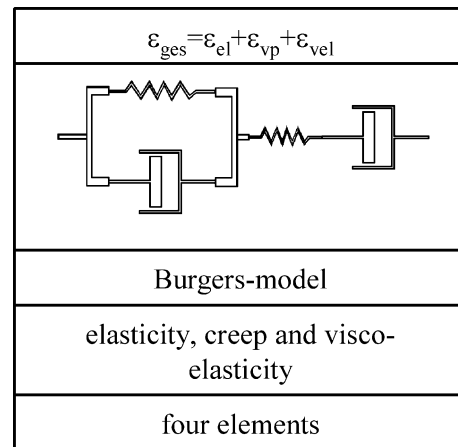


Fig. 6 Rheological model proposed for the deformation behaviour of epoxy materials

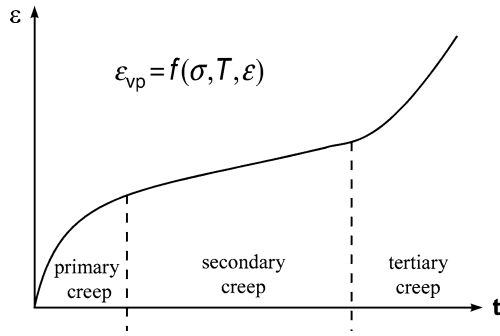


Fig. 7 Phases of viscoplasticity in a material

$$B = 1 - \frac{s}{s^*}, \quad s^* = \hat{s} \left[ \frac{\dot{\epsilon}}{A} e^{\frac{Q}{RT}} \right]^{n_s}$$

For modelling only the secondary part of creep, where the strain rate  $\dot{\epsilon}$  is constant, the model can be reduced to

$$\dot{\epsilon}_{cr} = C e^{-Q/RT} \sigma^n \quad (7)$$

#### 4 Simulation results

The following paragraphs describe simulation results, performed in order to investigate the stress distribution in the silicon chip after the backend-fabrication processes and the influence of temperature-dependent material data as well as the influence of geometry parameters. Only stresses in  $x$ -direction ( $\sigma_x$ ) are displayed. Due to symmetry, the stress in  $y$ -direction is in the same order of magnitude whereas stresses in  $z$ -direction are negligible in the cases simulated here.

##### 4.1 Simulating the backend-process

For simulating the backend fabrication process linear-elastic, temperature-dependent materials data were used, for the adhesive a viscoplastic model was used. The described material behaviour influences the sensor performance already during the backend fabrication process. Throughout the process, the device is exposed to various temperatures and temperature cycles. The glue dispensing is performed at room temperature (25°C). The glue-curing is carried out at a temperature of 145°C, after that, the device is cooled down to room temperature. The moulding and the mould-cure are executed at a temperature of 180°C. This can be followed by e.g. end-tests (Fig. 8).

The temperature-time-characteristics used in the simulations are reduced to the temperature-steps of the process, which seem relevant and are shown in Figs. 9 and 10.

During the glue-curing the device is almost stress-free (Fig. 12). While cooling down, the Young's modulus of the adhesive rises significantly and stress is induced in the device. The stress in the silicon top layer depends on

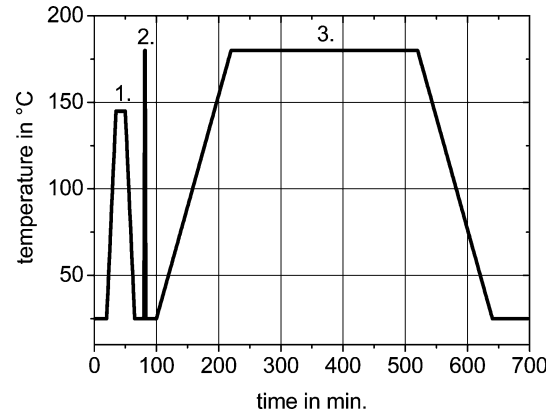


Fig. 8 Typical process temperatures during a backend fabrication process; 1 glue-curing, 2 moulding and 3 mould-cure

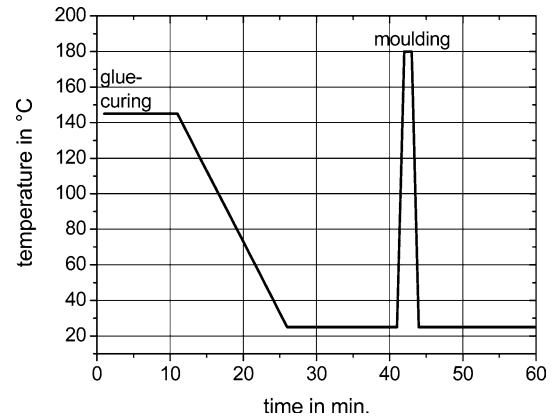


Fig. 9 temperature-time-profile used in the simulation

the change in temperature, the thickness of each material layer, the Young's moduli and the difference of the coefficients of thermal expansion. Because of a higher CTE of the leadframe tensile stresses in the silicon top layer can be observed (Figs. 10, 11).

Figure 12 shows the stress in the top layer of the silicon chip over the temperature cycle of glue-curing

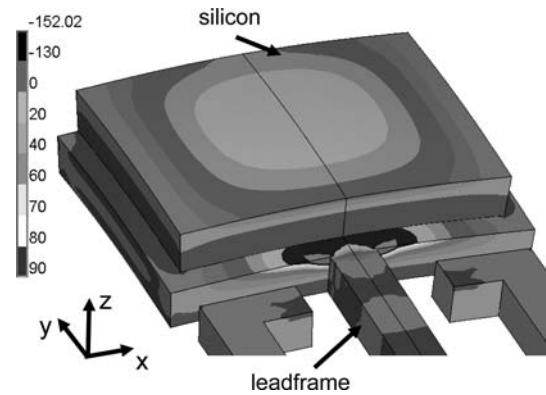
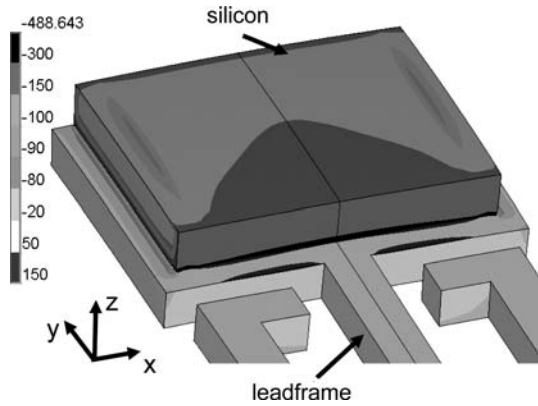


Fig. 10 Stress  $\sigma_x$  in the silicon-chip after the glue-curing and cooling down to 25°C and 1 h at 25°C



**Fig. 11** Stress  $\sigma_x$  in the silicon chip after mould-annealing and 1 h at 25°C. Moulding compound type a. The moulding compound was removed for visualization

and moulding. A change in the slope of the stress curve while cooling down the device after the gluing step can be observed at about 80°C, which corresponds to the glass transition temperature of the adhesive. When heating up the device after the gluing process for moulding and mould-curing, this stress is reduced to approximately 20 MPa (Fig. 12), because of a rather low temperature difference to the reference temperature and the adhesive's low Young's modulus. When cooling down the sensor after moulding, stress is induced in the silicon top layer again.

Due to the surrounding moulding compound, the stress is now compressive and in the same order of magnitude as the stress after the glue-curing process. In comparison to the stress  $\sigma_x$  after the glue-curing, the stress-gradient after the gluing and moulding is much lower. Figure 13 displays the stress  $\sigma_x$  after the entire temperature cycle described above. The stress distribution within the silicon shows a linear stress gradient through the silicon with a stress value of approximately 75 MPa at the silicon top layer.

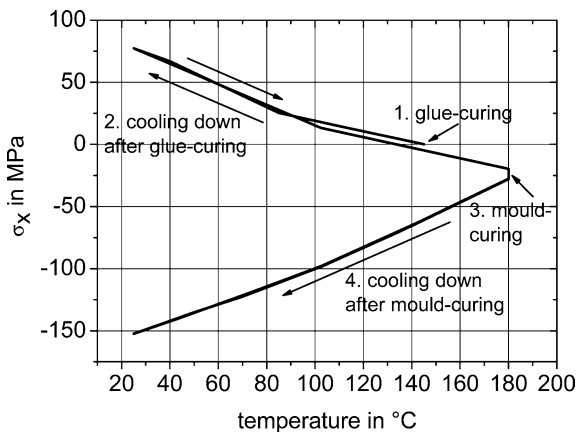


**Fig. 12** Stress in the top silicon layer while gluing and mould-curing the sensor device; moulding compound type a

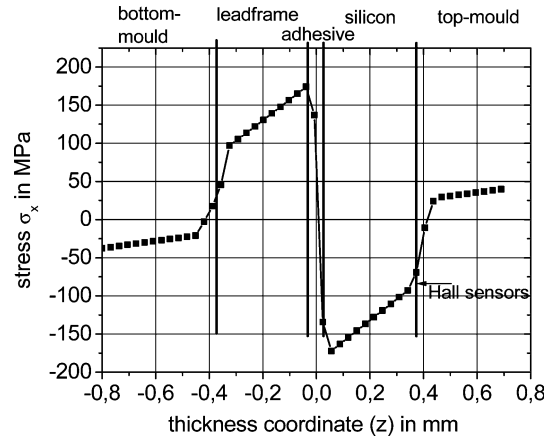


**Fig. 13** Stress  $\sigma_x$  in the sensor device along the thickness coordinate after glue-annealing and mould-annealing

## 4.2 Influence of moulding-shrinkage

Moulding compounds tend to shrink when heated up during the moulding and the mould-cure process. This behaviour influences the stress field in the sensor device and leads to a higher stress in the top silicon layer. Figure 14 displays the stress  $\sigma_x$  in the top silicon layer over the backend process when considering a shrinkage of the moulding compound of 0.5%. Compared to the results without considering shrinkage, 25% higher stress values in the top silicon layer are observed.

## 4.3 Influence of temperature-dependent material properties

Figure 15 shows the calculated stress distribution along the thickness coordinate in the middle of the silicon chip through a Hall sensor device, were linear-elastic and temperature-dependent materials data were used. When using a moulding compound with a glass-transition

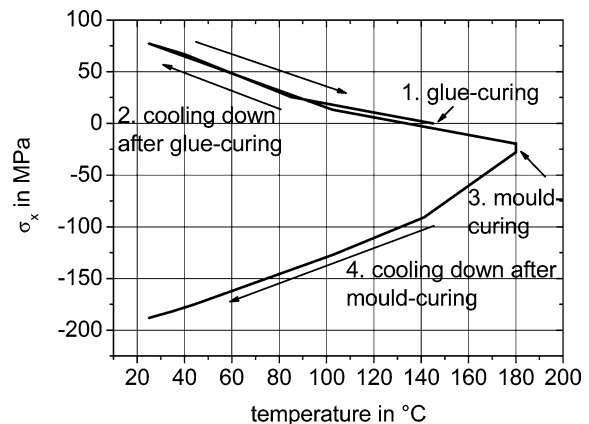


**Fig. 14** Stress in the top silicon layer of the sensor device while gluing and mould-curing, 0.5% shrinkage of moulding compound is considered, moulding compound type a

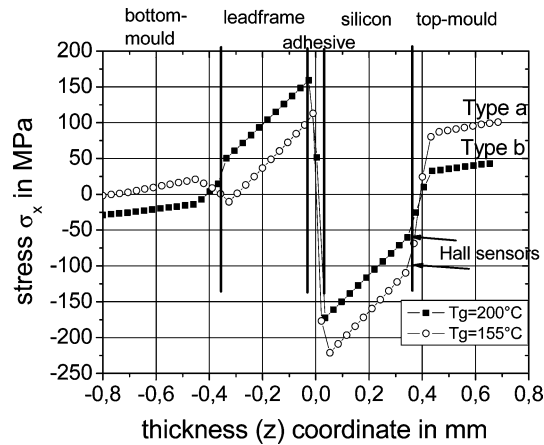


**Fig. 15** Stress distribution along the thickness coordinate within a leaded Hall sensor package. Comparison of two different moulding compounds (types a and b). Temperature drop from 180 to 25°C, linear-elastic simulation

temperature ( $T_g$ ) in the relevant temperature range the stress in the silicon top layer can be expected to be twice as high as with using a moulding compound with a  $T_g$  outside the relevant temperature range.

#### 4.4 Influence of geometry parameters

Table 2 displays the influence of a variety of geometric parameters on the stress induced in the silicon layer by a temperature change from 180 to 25°C. The simulations were performed linear elastically with temperature-dependent materials behaviour. For the conductive adhesive, a viscoplastic model was used. By decreasing e.g. the silicon thickness, the bending radius is decreased resulting in a higher stress in the top silicon layer.

## 5 Conclusion

It was the objective of this investigation to show that the offset and sensitivity of sensors is strongly influenced by the packaging material. To be able to predict this behaviour exactly, especially over many temperature cycles, models are needed which describe the highly complex material behaviour exactly. The performed simulations of moulded Hall sensor devices and measurements on moulding compounds show the following:

**Table 2** Influence of geometry parameters on the temperature-dependent stress in the active silicon layer, independent variations of the standard design simulated on the entire device, linear-elastic simulation with viscoplastic model for the adhesive

Parameter	Change of parameter	Maximum stress ( $\sigma_x$ ) in Hall plate
Standard		-130
Adhesive thickness	Higher than	-122
Silicon-chip thickness	Lower than	-230
Leadframe thickness	Lower than std.	-124
Top layer moulding thickness	Lower than std.	-34
Bottom layer thickness	Lower than std.	-136

- Geometry as well as temperature-dependent and time-dependent materials deformation will influence the stress field in a sensor device and thus the performance of the sensor, strongly.
- For simulating the entire backend fabrication process correctly, all temperature-dependent and time-dependent material properties must be considered.
- For MEMS-Hall sensors the offset and the sensitivity are highly dependent on the temperature and time-dependent material behaviour. The system behaviour can be optimized efficiently using finite elements simulations when the time-dependency and nonlinearity of the materials are taken into account.

## References

- Bittle DA, Suhling JC, Beaty RE, Jaeger RC, Johnson RW (1991) Piezoresistive stress sensors for structural analysis of electronic packages. *J Electron Packaging* 113:203–215
- Deier E, Wilde J (2003) Thermo-mechanical behavior of the die attachment adhesive of a MEMS pressure sensor. In: 14th European microelectronics and packaging conference and exhibition Friedrichshafen, Germany, 23–25 June 2003
- Fischer S, Wilde J, Deier E, Zukowski E (2004) Influence of materials data on the performance modelling in the design of MEMS packages. In: Symposium on advanced packaging, IEEE, 2004
- Hälg B (1988) Piezo-Hall coefficients of n-type silicon. *J Appl Phys* 64:276–282
- Manic D, Petr J, Popovic RS (2000) Short and long-term stability of Hall plates in plastic packages. In: IEEE, 38th international reliability physics symposium, San Jose, CA, 2000
- Wilde J, Deier E (2003) Einfluss des nichtlinearen Verhaltens der Montageklebung auf die Genauigkeit mikromechanischer Drucksensoren. In: Proceedings of the ninth GMM-workshop, Bielefeld, 31 March 2003/01 April 2003